Extended Abstracts of the 2001 International Conference on Solid State Devices and Materials, Tokyo, 2001, pp. 482–483

B-7-3

Mechanism of Improved Thermal Stability of B in Poly-SiGe Gate on SiON

Taizoh Sadoh, Fitrianto, Atsushi Kenjo, Akihiro Miyauchi[1], Hironori Inoue[1] and Masanobu Miyao
Department of Electronics, Kyushu University, 6-10-1 Hakozaki, Fukuoka 812-8581, Japan
Phone: +81-92-642-3952, FAX: +81-92-642-3974, E-mail: sadoh@ed.kyushu-u.ac.jp
[1]Hitachi Research Laboratory, Hitachi, 7-1-1 Omika, Hitachi 319-1292, Japan

1. Introduction

Poly-SiGe is a promising material for gate electrodes in the future ULSI because of the low resistivity and the ability of work function tuning. However, diffusion and deactivation of dopant atoms can be modulated significantly by the grain boundaries and Ge fraction. Consequently, the thermal stability of dopant atoms should be examined in order to establish the poly-SiGe films as ULSI materials. In line with this, post-annealing behavior of *in-situ* doped poly-SiGe layers on SiON films has been investigated.

2. Experimental Procedure

The SiON films (thickness: 2.5 nm) were grown on Si wafers. Subsequently, Si buffer layers (2 nm) and SiGe layers (70-180 nm) were deposited at 690℃ by the low-pressure CVD. During deposition, B_2H_6 was introduced into the chamber for *in-situ* doping of B. The flat B profile with the concentration of about 2×10^{20} cm^{-3} was confirmed by SIMS measurements. Finally, the samples were annealed at 600-900℃ for 5-5000 min in N_2. Carrier densities and concentration profiles were evaluated by using Hall effect measurements by the aid of anodic oxidation layer removal method.

3. Results and Discussion

Post-annealing characteristics of carriers at 800℃ are shown in Fig.1(a). With increasing annealing time, the carrier density decreases and converges to constant values. Figure 1(b) compares the carrier concentrations for as-deposited and annealed (10^3 min) samples. The thermal equilibrium solubility of B in poly-SiGe [1] is also shown. The results clearly indicate that the super-saturated concentration in the as-deposited films converges to the thermal equilibrium solubility during post-annealing. Figure 1(c) shows the annealing time at which 50% of initial carriers were deactivated. This indicates that the thermal stability of super-saturated electrically-active B is significantly improved by Ge doping. For example, the stability for $Si_{0.6}Ge_{0.4}$ is 4 times as high as that for Si.

Next, the deactivation process was analyzed. Figures 2(a) and 2(c) show semi-log plots of normalized carrier concentrations after annealing at 700 and 800 ℃, respectively. The deactivation process can be separated into fast process with time constant τ_1 (Figs.2(b) and 2(d)) and slow process with τ_2. These experimental data can be fitted to the following equation:

$$\frac{(N(t)-N_\infty)}{(N_0-N_\infty)} = \Delta N_1 \exp(-t/\tau_1) + \Delta N_2 \exp(-t/\tau_2), \quad (1)$$

where $N(t)$, N_0, and N_∞ are carrier concentrations at t, $t=0$, and $t=\infty$, respectively, and ΔN_1 and ΔN_2 the deactivated concentrations in the fast and slow processes, respectively.

Arrhenius plot of τ_2 is shown in Fig.3(a). Almost the same activation energy E_2 of 2.8 eV and pre-exponential factor f_2 of $\sim10^{10}$ sec^{-1} were obtained for all samples, where $1/\tau_2 = f_2 \exp(-E_2/kT)$. These values are compared with those for solid-phase growth of SiGe [2] in Fig.3(b). They agreed well each other. These results suggest that B deactivation in the slow process is due to B trapping at grain boundaries during grain growth. TEM observation confirmed that grain growth of poly-SiGe became significant in these annealing conditions. Figure 3(c) shows the plot of τ_1, which yields almost the same activation energy E_1 of 1.3 eV and pre-exponential factor f_1 of $\sim10^4$ sec^{-1} for all samples. This suggests that B deactivated in the fast process is due to B transition from substitutional to interstitial sites in the grains. However, Ge fraction dependence of the thermal stability (Fig.1(c)) could not be explained by the analysis of $\tau_1(E_1, f_1)$ and $\tau_2(E_2, f_2)$.

To solve this problem, we paid attention to the ratio of deactivated B concentration in the fast and slow processes, i.e., $\Delta N_1/\Delta N_2$. This ratio significantly decreases by Ge doping as shown in Fig.4. To understand these phenomena, we propose the two-state model as shown in Table I: B atoms exist in two states, i.e., B surrounded by only Si (state 1), and Si and Ge (state 2). In the state 1, a local strain is induced due to the difference of atomic radii between Si and B, so that B is easily swept out from substitutional sites. Such strain is compensated by Ge doping, and thus B in the state 2 becomes stable. With increasing Ge fraction, number of unstable B (state 1) decreases. On the other hand, the slow process (ΔN_2) is controlled by grain growth and almost independent of Ge fraction. In this way, $\Delta N_1/\Delta N_2$ decreases with increasing Ge fraction. This means that the stability of B is improved by Ge doping.

4. Summary

Post-annealing characteristics of *in-situ* B-doped poly-SiGe have been investigated. Thermal stability of B is significantly improved by Ge doping, e.g., the stability for $Si_{0.6}Ge_{0.4}$ is 4 times as high as that for Si. The deactivation process of B consists of the fast and slow processes. The time constants for both processes do not depend on the Ge fraction, while the ratio of deactivated B in the fast process to that in slow process decreases by Ge doping. The two-state model has been proposed, and explained the improved thermal stability of B by Ge doping.

References

[1] P.-E. Hellberg, et al., J. Electrochem. Soc. 144 (1997) 3968.

[2] P. Kringhoj, et al., Nucl. Instrum. Methods B 106 (1995) 346.

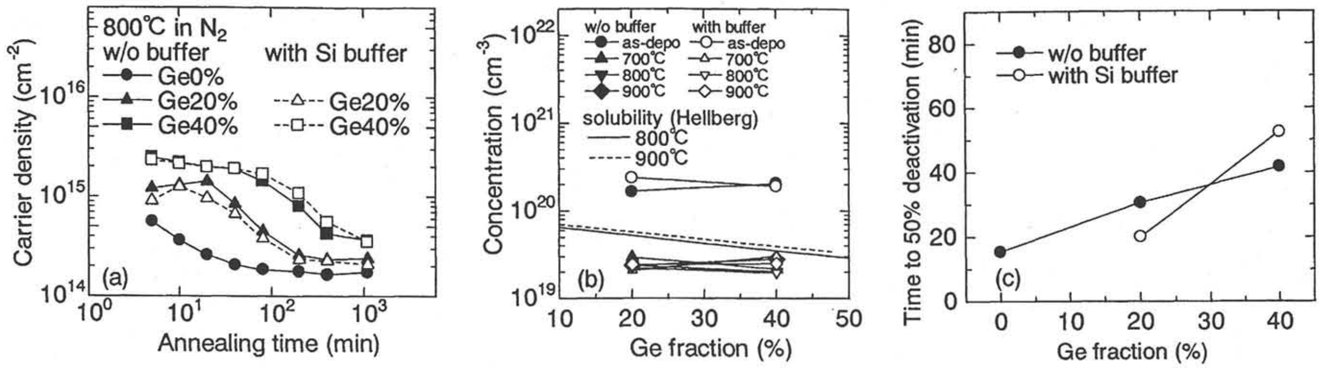

Fig.1 Isothermal annealing characteristics of carriers at 800℃ (a) and Ge fraction dependence of carrier concentration for as-deposited and annealed ($\sim 10^3$ min) samples (b) and time to 50% deactivation (c). The data of solubility of B in poly-SiGe [1] are also shown in (b).

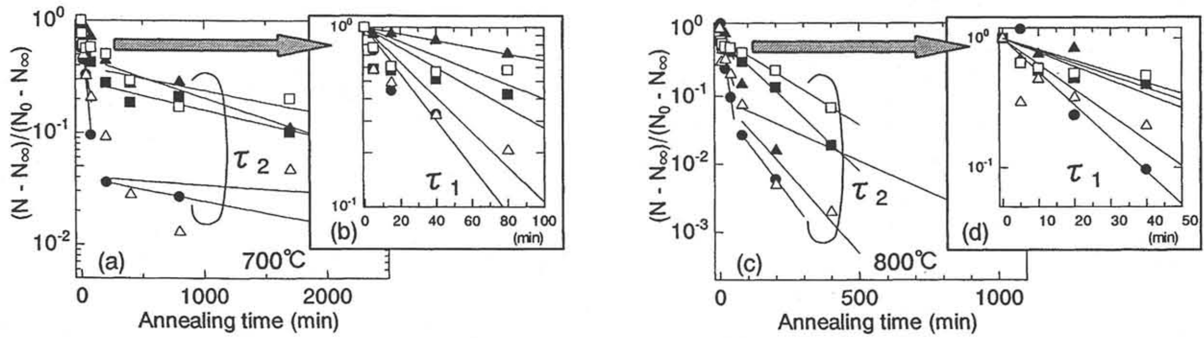

Fig.2 Annealing characteristics of normalized carrier concentration at 700 (a) and 800℃ (c). The characteristics in the initial stage are magnified in (b) and (d). The notations for samples are same as those in Fig.1(a).

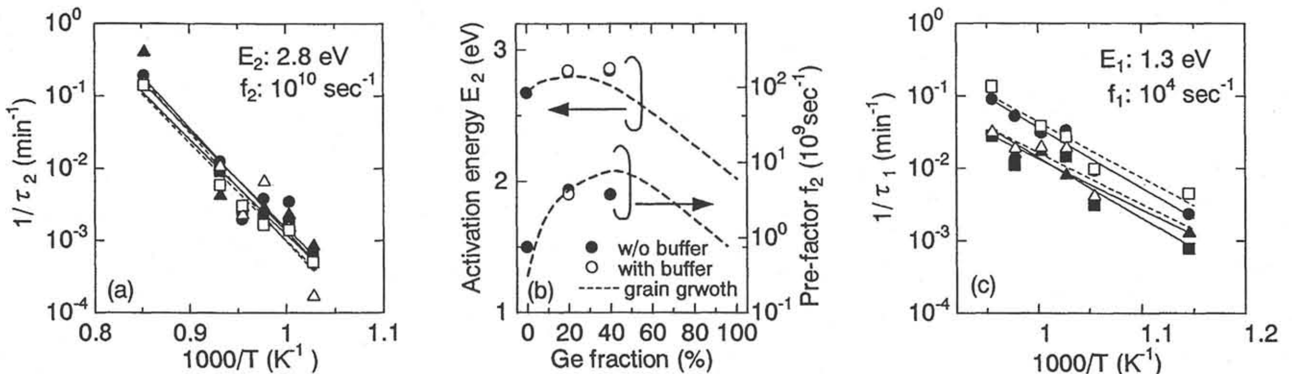

Fig.3 Arrhenius plot of τ_2 for slow process (a), Ge fraction dependence of activation energy and pre-exponential factor for τ_2 (b), and Arrhenius plot of τ_1 for fast process (c). The data of solid-phase growth of SiGe [2] are also shown in (b).

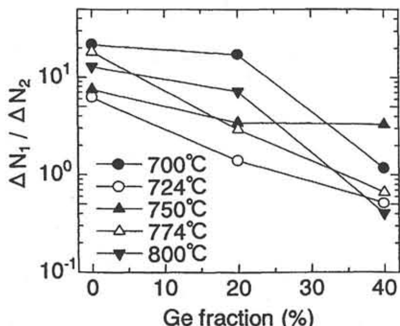

Fig.4 Ge fraction dependence of ratio of concentration deactivated in fast process to that in slow process.

Table I Two-state model for improved thermal stability of B by Ge doping.

	Fast Process (ΔN_1)	Slow Process (ΔN_2)
State 1 (Si - B - Si, with Si above and below B)	B deactivation (substitutional to interstitial sites) by local strain.	B trapping during grain growth
State 2 (Si - B - Ge, with Si above and below B)	B stabilization by local strain compensation	

Atomic radius: 1.17A (Si), 1.22A (Ge), 0.81A (B)